

Final Draft
of the original manuscript:

Homaeigohar, S.; Koll, J.; Lilleodden, E.T.; Elbahri, M.:

**The solvent induced interfiber adhesion and its influence on the
mechanical and filtration properties of polyethersulfone
electrospun nanofibrous microfiltration membranes**

In: Separation and Purification Technology (2012) Elsevier

DOI: 10.1016/j.seppur.2012.06.027

The solvent induced interfiber adhesion and its
influence on the mechanical and filtration
properties of polyethersulfone electrospun
nanofibrous microfiltration membranes

Shahin Homaeigohar^a, Joachim Koll^a, Erica Thea Lilleodden^c,
and Mady Elbahri^{a,b*}

a: Helmholtz-Zentrum Geesthacht, Institute of Polymer Research, Nanochemistry and
Nanoengineering group, Max-Planck-Str. 1, 21502 Geesthacht, Germany

b: Nanochemistry and Nanoengineering group, Institute for Materials Science, Faculty
of Engineering, University of Kiel, Kaiserstrasse 2, 24143 Kiel, Germany

c: Helmholtz-Zentrum Geesthacht, Institute of Materials Research, Max-Planck-Str. 1,
21502 Geesthacht, Germany

* To whom correspondence should be addressed:

E-mail: mady.elbahri@hzg.de

Abstract

Electrospun nanofibrous membranes (ENMs) as a novel class of energy saving membranes are under extensive investigation. This kind of membranes are highly porous and permeable however mechanically weak. In the current study, we benefited the residual solvent of the electrospun nanofibers to induce an interfiber adhesion through a thermal treatment. This approach was successful in enhancement of the mechanical properties of the electrospun nanofibrous membrane probed via tensile test and nanoindentation as a higher elastic modulus and compaction resistance, respectively. The mechanically stronger membrane possesses a higher resistance against tensile disintegration thereby a lower water flux at high feed pressures. Through a particle challenge test i.e. filtration of a TiO₂ aqueous nanosuspension under an incremental feed pressure of 1-2 bar, we could also show that a mechanically resistant ENM can offer a more optimum filtration efficiency mainly due to its higher structural integration.

Keywords: electrospinning, nanofibrous membranes, water filtration, mechanical properties

1. Introduction

One of the most well-known production techniques of continuous sub-micron to nano-size fibers is “electrospinning” [1]. Electrospun nanofibrous mats are highly porous with interconnected pores as big as only a few times to a few ten times the fiber diameter. The promising structural features make them a suitable candidate for filtration applications. The high porosity implies a higher permeability and the interconnected pores can withstand fouling better. Moreover, small tunable pore size of the nanofibrous non-wovens brings about a high retention [2].

In separation technology, application of electrospun nanofibrous mats can be classified into three major areas: gas, liquid and molecular filtration. As air filters, electrospun nanofibrous non-wovens have been used commercially over the last 20 years [2]. However, in other filtration areas the research is extensively being done to meet the requirements for industrialization of such nanofibrous filters.

Recalling very high porosity and surface area to volume ratio of the electrospun nanofibrous membranes (ENMs), one of the main industrial requirements is their mechanical stabilization. Despite promising filtration features, however, an electrospun membrane which is exposed to various stresses applied by e.g. a liquid flow should also possess enough mechanical stability. Indeed, for liquid filtration applications, besides chemical stability a membrane needs to be mechanically strong enough in order to efficiently separate particulates from liquid streams such as water, hydraulic fluids, lubricant oils or fuels [3, 4].

In the current research, an electrospun polyethersulfone (PES) nanofibrous mat is considered as a candidate for liquid filtration. PES was selected as the membrane material due to its high thermal and chemical resistance, also its appropriate mechanical properties. Furthermore, PES can be considered as a model

membrane material as it is widely used for commercial microfiltration and ultrafiltration membranes. In a previous study, the filtration performance of this membrane was evaluated through water flux measurement and retention test [5]. The results showed promising filtration abilities of this membrane for pre-treatment of water, however to assess its industrial scale filtration potential, its mechanical performance and stability during filtration should also be investigated and optimized, respectively.

To mechanically stabilize electrospun nanofibrous membranes, an efficient nanocomposite strategy was recently employed by our group [6, 7]. In a new study, we aim to investigate another approach, that is the solvent induced interfiber adhesion through a heat treatment process. This approach could be very simple and more cost and time efficient than the other previously attempted strengthening methods e.g. composite technology. Moreover, the porous structure i.e. pore size is assumed not to change significantly.

Thermal treatment at a temperature above glass transition temperature and just below melting temperature of the polymeric nanofibers is a well-known approach to strengthen a nanofibrous mat [8]. Different from such a successful technique, we benefited heating in extracting residual solvent from within the nanofibers. The residual solvent can act as a glue to partially dissolve and stick the nanofibers to each other. This interfiber adhesion is assumed to increase the mechanical properties of the nanofibrous membrane without a significant change in the porous structure.

In the current study, we aim to optimize the mechanical stability of a PES ENM through a solvent induced interfiber adhesion technique. Efficiency of this approach is investigated at different mechanical conditions of compressive and tensile by nanoindentation and tensile test, respectively. Moreover, the membranes were

evaluated via a water flux and retention test under incremental feed pressures to prove the positive effect of the adopted strengthening approach on filtration performance of the PES ENMs.

2. Experimental

2.1. Material

Polyethersulfone Ultrason E6020P ($M_w = 58,000$ and density of 1.37 g/cm^3) was purchased from BASF (Germany). The solvent *N,N*-dimethylformamide (DMF) was obtained from Merck (Germany). Titania nanoparticles as a model for colloidal nanoparticles to be filtered out by the ENMs, were also obtained from Degussa (Japan). All materials were used as received.

2.2. Electrospinning and heat treatment

PES nanofibrous mats were produced by an electrospinning method. Briefly, a prepared PES solution (20 wt%) in *N,N*-dimethylformamide (DMF) was fed with a constant rate of 0.5 ml/h into a needle by using a syringe pump (Harvard Apparatus, USA). By applying a 20kV voltage (Heinzinger Electronic GmbH, Germany) PES was electrospun on an aluminium foil located 25 cm above the needle tip for 8 hours.

After peeling off the aluminium foil, the electrospun nanofibrous mats were prepared as two groups; untreated and heat treated. As the latter group, the samples were heated in the oven (Heraeus Vacutherm, max $T=200^\circ\text{C}$) at the temperature of 190°C for 6 hours in air and then were slowly cooled in the oven.

2.3. Morphological characterization of the PES nanofibrous mats

The morphology of the PES electrospun nanofibers was observed through scanning electron microscope (SEM) (LEO 1550VP Gemini from Carl ZEISS) after a gold coating. The diameter of the nanofibers was determined from the SEM images using the Adobe Acrobat v.07 software. The thickness of the PES nanofibrous mats for all the mechanical tests was measured using a digital micrometer (Deltascope® MP2C from Fischer).

2.4. Nanoindentation

Nanoindentation tests were conducted using a Nanoindenter XP (MTS system Co., MN, USA) with a continuous stiffness measurement (CSM) technique. A conical diamond flat punch indenter with diameter of 50 μm and angle of 60° was used for the tests.

All nanoindentation tests were performed at room temperature. The CSM technique is carried out by introduction of a small, sinusoidal varying force on top of the applied linear force driving the motion of the indenter. The displacement response of the indenter to the sinusoidal force at the excitation frequency (45 Hz in this study) is measured continuously as a function of the indentation depth (~ 10% of the membrane thickness) [9, 10]. As such, the dynamic mechanical properties changing with respect to the indentation depth can be obtained.

The nanoindentation tests were carried out as follows: a displacement rate of 100 nm/s was maintained constant during the increment of load until the indenter reached 10,000 nm deep into the surface of the membrane mounted on a SEM stub. After that, the load was kept at maximum value for 10 s to inhibit the effect of creep on the unloading behavior [11]. The increasing displacement of the indenter while

holding the load at maximum value represents the creep of the ENMs. The indenter was then withdrawn from the surface at the unloading rate of 0.1 mN/s. At least 10 indents were performed on each sample and the distance between the indentations was 200 μm to avoid interaction.

2.5. Tensile test

Rectangular stripes of the PES nanofibrous mats (10 mm x 80 mm x 140 μm) were carefully cut and stretched by a tensile machine (Zwick/Roell Z020-20KN, Germany) equipped with a 20-N load-cell at ambient temperature. The cross-head speed was 2 mm/min and the gauge length was 20 mm. The reported tensile moduli, tensile strengths and elongations represented average results of ten tests.

2.6. Bubble point test

To assess any eventual change in the porous structure after heat treatment, average pore size of the electrospun nanofibrous membranes was measured using an automated capillary flow porometer from Porous Materials Inc.(PMI,USA). The details of this characterization can be found at [5].

2.7. Pure Water flux measurement

Membrane permeability versus feed pressure was characterized through a pure water dead-end filtration (the set-up shown in Fig.1). The PES ENMs as un- and heat treated were mounted on a poly(*p*-phenylene sulfide)(PPS) non-woven sub layer to prevent an intimate contact with the metal sieve of the membrane module and pore clogging. The dried hybrid membrane (active filtration area $\sim 2 \text{ cm}^2$) was placed in the membrane module and the water in the reservoir (125 ml) was passed through by

applying feed pressures of 1-2 bar with an increment of 0.5 bar. The time required for permeation of the water through the membranes was recorded and the flux according to the equation (1) was calculated :

$$J = \frac{Q}{A \cdot \Delta t} \quad (1)$$

where J is the water flux ($L/m^2 \cdot h$), Q is the permeated volume of water (L), A is the effective area of the membranes (m^2), and Δt is the sampling time (h). The flux measurement tests were repeated three times.

2.8. Retention test

The retention capability of the PES ENMs (already mounted on a PPS non-woven sub layer) at various feed pressures was determined using TiO_2 aqueous nanosuspensions.

The dried hybrid membranes were placed in the membrane module of the custom-built set-up (Fig. 1) and by applying various feed pressures of 1-2 bar (with increment of 0.5 bar), 100 mL TiO_2 heterodisperse suspension (0.04 g/L) as the feed was passed through. The average particle size of the feeds and permeates was determined by using a particle size analyzer (Delsa C TM Nano particle size analyzer, Beckman Coulter, USA). Moreover, to calculate the permeate flux according to the equation (1), the permeation time was also recorded.

3. Results and Discussion

3.1. Characterization of the PES nanofibrous mats

The morphology of the electrospun nanofibers is shown in Fig. 2. The surface of the nanofibers is relatively smooth and the nanofibers have a diameter of approximately 200 ± 60 nm.

From SEM images of the electrospun PES nanofibers (Figs. 2 A and B), the fiber junction points in the heat treated nanofibrous mat appeared to be jointed more closely with some even slightly fused together, as compared to those in the untreated membranes. The selected temperature for the heat treatment (190 °C) is above the boiling point of the solvent ($T_b(\text{DMF})=153$ °C) and below the glass transition temperature of PES (225 °C). It is assumed that the residual solvent in the nanofibers (2.5% as measured by TGA in [5]) can partially re-dissolve PES by heating. Continuous heating results in diffusion of the solution outward of the nanofibers to the interface with the other nanofibers. By evaporation of the solvent at the interface, the nanofibers stick to each other firmly.

3.2. Nanoindentation

The heat treatment approach as mentioned earlier could be positively influential on mechanical stability of the electrospun nanofibrous membranes. The probable improvement of the mechanical properties of the PES ENM under compressive forces e.g. as a higher compaction resistance was investigated through a nanoindentation test.

Fig. 3A represents a typical load-displacement graph obtained by the nanoindentation test for the PES electrospun nanofibrous mats as un- and heat treated.

According to the load-displacement graph, the compaction index of the PES ENMs can be defined by the equation (2):

$$I_C = \left(1 - \frac{h_{\max} - h_f}{h_{\max}}\right) \times 100\% = \frac{h_f}{h_{\max}} \times 100\% \quad (2)$$

where, h_{\max} and h_f represent the displacements at peak load and after complete unloading, respectively. The calculated compaction indices are presented in Fig. 3B. It is seen that the heat treated ENMs show a lower compaction index compared to the untreated ones. The bigger error bars seen for the untreated ENM implies non-homogeneity of the nanofibrous mat in term of the mechanical resistance.

Besides the compaction index, the storage modulus (E') of the electrospun nanofibrous mats can be inferred from the initial unloading contact stiffness (S), i.e. the slope of the initial portion of the unloading curve by following the equation (3) [11-13]:

$$E' = \frac{\sqrt{\pi}}{2\beta} \frac{S}{\sqrt{A}} \quad (3)$$

where β is a constant that depends on the geometry of the indenter ($\beta = 1$ for a flat punch indenter). The calculated values of E' for the untreated and heat treated ENMs are presented in Fig. 3B. The assumption for measuring storage modulus as above (Oliver-Pharr method) is based on the concept that primary unloading should be prevailed by the linear elastic recovery. To meet this condition i.e. minimizing the viscoelasticity effect, the load should be kept constant at the end of the loading part for a short given time (holding time) or a high load/unloading rate is implemented. Otherwise even during the unloading part, there would be some continued deformation (often identified as a “nose” in the force curve) i.e., the penetration depth is still increasing while the load is decreasing. This assumption is one of the major drawbacks of this method for evaluation of elastic modulus for polymeric materials

[14]. Therefore, the presented results cannot be accurate and show only the general trends.

On the whole, surprisingly, a higher elastic modulus is observed for the untreated membranes as compared to the heat treated ones. The probable reasons should be sought in the following instances:

1- Pore collapse and compaction during loading on the electrospun nanofibrous membrane which results in a higher density and lower porosity. Similar behavior has been reported by Kucheyev et al.[15].

According to Lu et al. [16] and Pal [17], the effective elastic modulus for a highly porous structure such as an electrospun nanofibrous membrane can be expressed by the equation (4):

$$E = E_m(1 - \phi)^2 \quad (4)$$

where E and E_m stand for the effective elastic modulus of the porous (with porosity of ϕ) and bulk material respectively. Decrease of porosity through applied load and compaction of the nanofibrous layer result in a higher elastic modulus in the membranes. The heat treatment preserves the porosity more as compared to the untreated membranes and this is why the elastic modulus of the heat treated sample is lower than that of the untreated one.

Additionally for the low density solids with relative densities $\rho^* \leq 10\%$, the elastic modulus follows the equation $E \approx (\rho^*)^m$, in which depending on the composition and morphology $m \approx 3-4$ [15]. Hence, E increases very rapidly (superlinearly) with compaction and relative density.

2- Van der Waals interaction of high aspect-ratio nanofibers (nanofiber sliding) during deformation [15]. Higher movement of the untreated nanofibers results in

their higher interactions and consequently a higher resistance to penetration of indenter.

3- Dissipative movement of air filling the pore volume [15].

4- Indenter friction with sliding nanofibers [15]

The energy dissipation during loading-unloading can be estimated by measuring the area confined between load-unload curves [11]. Based on our measurements, plastic work for the untreated and heat treated ENMs are 13.5 and 9 nN.m, respectively. These values show the untreated ENM undergoes a higher plastic deformation. Kucheyev et al. [15] state that two possible mechanisms for energy dissipation in highly porous solids can be (i) van der Waals interaction of high aspect-ratio nanoligaments (nanofibers in our study) due to their sliding during deformation and (ii) dissipative movement of air filling the pore volume.

The hold time at the maximum load was used to show the creep effect of the electrospun nanofibrous mats. Increase of displacement (indentation depth) at the maximum load represents the creep. As can be seen in Fig. 3C, the creep effect was more apparent in the case of the untreated nanofibrous mats. In polymeric materials, cross linking of the polymer chains decreases the amount of creep [18], similarly, here also the physical interfiber bonding of the nanofibers due to heat treatment results in a lower creep for the heat treated nanofibrous mats.

3.3. Tensile test

Enhancement of tensile mechanical properties of the PES ENM after the heat treatment was also probed via a tensile test. The typical tensile stress-strain curves for the PES electrospun nanofibrous mats are shown in Fig. 4A. Furthermore, the

measured values of the tensile mechanical properties of these nanofibrous mats are presented in Fig. 4B.

As can be seen in Fig. 4A, for the untreated nanofibrous mat, stress increases gradually up to the peak and then decreases with a similar trend. In contrary, stress variation versus strain results in a steep slope for the heat treated ENM indicating an increase in the tensile modulus and strength with a concurrent decrease of the elongation to break. This behavior can be explained as follows: the untreated nanofibers can easily slide by one another during tensile deformation, resulting in low tensile strength and high elongation. However, for the heat treated nanofibrous mats, the nanofibers firmly adhered to each other can not slide freely. In other words, the interfiber bonding limits the stretchability of the membrane and makes the nanofibrous mat more rigid. Therefore, the heat treated nanofibrous mat had higher tensile modulus and strength and lower elongation at break (Fig. 4B).

Similarly, such a performance has been reported by other researchers [8, 19]. In such studies based on a different principle with our residual solvent based approach, the mat is heated up to a temperature above glass transition temperature and just below melting point. This temperature may be even lower than T_b of the residual solvent e.g. in the case of PVDF nanofibrous mat with DMAc solvent [20]). Through fusing the nanofibers to each other the nanofibrous web becomes rigid and mechanically stronger.

The mechanical characterizations implied compaction of both the un- and heat treated ENMs but with a lower amount for the latter group. Moreover, while tensile stretching, the heat treated ENM shows a significantly higher resistance to

disintegration i.e. an unchanging porous structure. Such performances could be influential on filtration efficiency of the PES ENMs.

3.4. Pore size measurements

As seen in Fig. 5, according to the bubble point test, both the PES ENMs possess a bubble point and mean flow pore diameter in the range of microfiltration (0.1-10 μm)[21] and comparable. This means that the heat treatment does not change the pore size of the membranes significantly. Moreover, in term of filtration, the membranes should be considered as microfiltration membranes able to perform under a feed pressure up to 2 bar [22]. Hence, we examined the ENMs' performance after the heat treatment in terms of water flux and retention test at feed pressures of 1-2 bar with an increment of 0.5 bar.

3.5. Water flux measurements

Mechanical performance of the ENMs can affect on their permeance behaviour.

According to the Darcy's law (equation (5)), increase of the feed pressure should increase water permeability directly [23, 24]:

$$J = \frac{k}{\mu} \left(\frac{\Delta P}{\Delta x} \right) \quad (5)$$

where J is the water flux (m^3/s), k the permeability coefficient (m^2), ΔP the pressure difference across the membrane (Pa) ($1 \text{ Pa} = 10^{-5} \text{ bar}$), μ the dynamic viscosity (Pa s) and Δx the membrane thickness (m).

As shown in Fig. 6, however, for the two groups of the membranes ascending trend of water flux is different with a higher rate for the untreated ENM. Such a significantly higher water flux rate could be attributed to the less resistance and more

susceptibility to disintegration of the untreated nanofibrous mat as proved via tensile test as well. Figs. 7 A-D show the appearance of the PES ENMs at a low magnification before and after a water flux test under a 2 bar feed pressure. Disintegration of the nanofibrous layer for both the ENMs is clearly evident. However, according to the water flux test results a less disintegration is assumed for the heat treated one.

3.6. Retention test with particle suspensions

Besides water permeance, the mechanical stability of the ENMs can be also influential on their filtration performance e.g. retention of suspended solids. Our membranes are considered as microfiltration membranes, hence they were evaluated with a TiO₂ particle suspension simulating real feed aqueous suspensions containing heterodisperse submicron inorganic particles.

For the retention test of whether un- or heat treated PES ENMs, two feed TiO₂ suspensions with almost equal average particle size (700 nm) were selected. The results of the retention tests judged by the average particle size of the feeds and permeates as well as permeability (permeate flux) of the PES ENMs are presented in Figs. 8 A,B, respectively.

As seen in Fig. 8A, at the feed pressures of 1 and 1.5 bar, in contrary to the untreated ENM, the heat treated one is able to catch all the nanoparticles. The cake layer gradually being formed protects the membrane from disintegration. Hence, the heat treated membranes can survive and reject the nanoparticles efficiently. However, at the highest feed pressure, either disintegration occurs very soon not letting a dense and integrated cake layer forms or the cake layer formed on the heat treated ENM is not able to resist against water flow and breaks up which subsequently leads to

disintegration of the membrane and passing the nanoparticles through the membrane (Fig. 8A) with a high permeability (Fig. 8B). As seen in Figs. 8A&B, this situation occurs much sooner for the untreated ENM at the feed pressure of 1 bar. Low rejection and high permeability of this membrane testifies this reality. Figs. 9 A-D show the cake layer formed on the heat and untreated PES ENMs at the feed pressures of 1 and 2 bar.

Permeability behaviour of the ENMs as presented in Fig. 8B depends upon the cake layer resistance and feed pressure and can be explained in a quantitative manner by the Darcy's law (equation (6))[25]:

$$J = \frac{\Delta P}{R_{tot} \mu} \quad (6)$$

Where R_{tot} is the total hydraulic resistance and μ the viscosity of the permeate.

R_{tot} can be defined as the sum of two contributions caused by the membrane (R_{mem}) and cake layer (R_{cake}). So, if according to the mechanical tests, we assume a higher resistance for the heat treated ENMs, a higher flux is expected for the untreated ENMs. This performance previously was shown by the water flux test.

The Kozeny-Carman equation (equation (7)) can be used for calculation of the cake layer resistance[25, 26] :

$$R_{cake} = \frac{180(1-\varepsilon)^2}{d_p^2 \varepsilon^3} \delta_c \quad (7)$$

where ε is the cake's void fraction (as low as 0.18 for polydisperse systems), δ_c the cake layer thickness and d_p the particle diameter.

The higher permeability for the untreated membranes throughout the retention test is attributed primarily to the less membrane resistance which can subsequently lead to a smaller cake resistance as well (lower δ_c).

On the other hand it is assumed that at higher feed pressures the nanoparticles could collide each other and grow (d_p), the cake layer formed consists of the particles with bigger diameter thereby with a lower resistance. This feature could lead to a higher permeability at the higher feed pressures.

On the whole, although the heat treated ENM showed a less permeability than its untreated counterpart mainly owing to its higher resistance to the liquid stream, it could be more efficient in rejection of the nanoparticles as long as not failed at the highest feed pressure.

4. Conclusion

Extraordinary interconnected porosity for the electrospun nanofibrous membranes from one hand brings about a very high permeability thereby very low energy consumption but on the other hand leads to their mechanical weakness. For industrialization, the effective electrospun nanofibrous membranes should be mechanically stable during different kinds of liquid filtrations.

In our study, the focus was on such an objective i.e. mechanical stabilization of a PES ENM without a significant change in the porous structure. To do so, a solvent induced interfiber adhesion approach was taken based on a heat treatment. The heat treated membranes were not that different with the untreated ones in term of pore size i.e. sustaining the same porous structure. But, they possessed a more optimum mechanical performance such as a better compaction resistance and tensile properties. Water flux test clearly proved that the heat treated ENM is more resistant and undergoes less disintegration than the untreated one reflected as a lower flux. Thanks to the less disintegration tendency before the highest applied feed pressure i.e. 2 bar, the heat treated ENMs also showed a much better retention efficiency for the

colloidal nanoparticles although with a less permeability due to a dense cake layer formation.

5. Acknowledgement

The authors would like to appreciate the financial support from a Helmholtz-DAAD PhD fellowship for Sh. Homaeigohar. M. Elbahri would like to thank The Initiative and Networking Fund of the Helmholtz Association for providing the financial base for the start-up of his research group. Additionally, the authors acknowledge the contribution of Dr. Katrin Ebert, formerly of the institute of Polymer Research, during the conception of this project, Prof. Volker Abetz for his useful discussions and comments on the mechanical characterizations also manuscript, Heinrich Böttcher for tensile tests, Kristian Bühr for design of the filtration set-up, Usman Zillohu, Sabrina Bolmer and Karen Prause for SEM pictures, respectively.

6. References

- [1] Z.M. Huang, Y.Z. Zhang, M. Kotaki, S. Ramakrishna, A review on polymer nanofibers by electrospinning and their applications in nanocomposites, *Compos. Sci. Technol.*, 63 (2003) 2223–2253.
- [2] C. Burger, B.S. Hsiao, B. Chu, Nanofibrous materials and their applications, *Annu. Rev. Mater. Res.*, 36 (2006) 333–368.
- [3] K. Yoon, B.S. Hsiao, B. Chu, Formation of functional polyethersulfone electrospun membrane for water purification by mixed solvent and oxidation processes, *Polymer*, 50 (2009) 2893-2899.

- [4] Sh. Homaeigohar, M. Elbahri, Nano Galaxy- a novel electrospun nanofibrous membrane, *Mater.Today*, In press (2012).
- [5] S.Sh. Homaeigohar, K. Buhr, K. Ebert, Polyethersulfone electrsopun nanofibrous composite membrane for liquid filtration, *J. Membr. Sci.*, 365 (2010) 68-77.
- [6] S.Sh. Homaeigohar, H. Mahdavi, M. Elbahri, Extraordinarily water permeable sol gel formed nanocomposite nanofibrous membranes, *J. Colloid Interface Sci.*, 366 (2012) 51-56.
- [7] S.Sh. Homaeigohar, M. Elbahri, Novel compaction resistant and ductile nanocomposite nanofibrous membranes with superior water permeability, *J. Colloid Interface Sci.*, 372(2012) 6-15.
- [8] S.S. Choi, S.G. Lee, C.W. Joo, S.S. Im, S. Kim, Formation of interfiber bonding in electrospun poly(etherimide) nanofiber web, *J. Mater. Sci.*, 39 (2004) 1511-1513.
- [9] W.C. Oliver, G.M. Pharr, An improved technique for determining hardness and elastic modulus using load and displacement sensing indentation experiments, *J. Mater. Res.*, 7 (1992) 1564-1583.
- [10] X. Li, B. Bhushan, A review of nanoindentation continuous stiffness measurement technique and its applications, *Mater. Character*, 48 (2002) 11-36.
- [11] B. J. Briscoey, L. Fiori, E. Pelillo, Nanoindentation of polymeric surfaces, *J. Phys. D: Appl. Phys.*, 31 (1998) 2395–2405.
- [12] G.M. Pharr, Measurement of mechanical properties by ultra-low load indentation, *Mat. Sci. Eng.*, A253 (1998) 151–159.
- [13] G.M. Odegard, T.S. Gates, H. Herring, Characterization of viscoelastic properties of polymeric materials through nanoindentation, *Exper. Mech.*, 45 (2005) 130-136.
- [14] D. Tranchida, S. Piccarolo, J. Loos, A. Alexeev, Mechanical characterization of polymers on a nanometer scale through nanoindentation. A study on pile-up and viscoelasticity, *Macromolecules*, 40 (2007) 1259-1267.
- [15] S.O. Kucheyev, A.V. Hamza, J.H. Satcher Jr, M.A. Worsley, Depth-sensing indentation of low –density brittle nanoporous solids, *Acta Mater.*, 57 (2009) 3472-3480.
- [16] G. Lu, G.Q. Lu, Z. Xiao, Mechanical properties of porous materials, *J. Por. Mater.*, 6 (1999) 359-368.
- [17] R.Pal, Porosity-dependence of Effective Mechanical Properties of Pore-solid Composite Materials, *J. Compo. Mater.*, 39 (2005) 1147-1158.
- [18] E.N. Lawrence, F. Robert, *Mechanical Properties of Polymers and Composites*, Marcel Dekker, New York, 1994.
- [19] Z. Ma, M. Kotaki, S. Ramakrishna, Surface modified nonwoven polysulphone (PSU) fiber mesh by electrospinning: A novel affinity membrane, *J. Membr. Sci.*, 272 (2006) 179-187.
- [20] R. Gopal, S. Kaur, Z.W. Ma, C. Chan, S. Ramakrishna, T. Matsuura, Electrospun nanofibrous filtration membrane, *J. Membr. Sci.*, 281 (2006) 581-586.
- [21] R. Baker, *Membrane technology and applications*, 2nd edition ed., Wiley, 2004.
- [22] S. Ramakrishna, R. Jose, P.S. Archana, A.S. Nair, R. Balamurugan, J. Venugopal, W.E. Teo, Science and engineering of electrospun nanofibers for advances in clean energy, water filtration, and regenerative medicine, *J. Mater. Sci.*, 45 (2010) 6283-6312.
- [23] Z. Wang, D.Z. Liu, W.J. Wu, M. Liu, Study of dead-end microfiltration flux variety law, *Desalination*, 201 (2006) 175-184.
- [24] P. Gibson, H. Schreuder-Gibson, D. Rivin, Transport properties of porous membranes based on electrospun nanofibers, *Colloid Surf. A-Physicochem. Eng. Asp.*, 187 (2001) 469-481.

[25] I.H. Huisman, D. Elzo, E. Middelink, A.C. Tragardh, Properties of the cake layer formed during crossflow microfiltration, *Colloid Surf. A-Physicochem. Eng. Asp.*, 138 (1998) 265-281.

[26] F.A.L. Dullien, *Porous Media, Fluid Transport and Pore Structure*, 1979.

Figure captions

Figure 1. Permeation set-up used for the water flux measurements

Figure 2. SEM micrographs showing formation of physical interfiber bondings after heat treatment :A) the untreated nanofibers; B) the heat treated nanofibers

Figure 3. Nanoindentation results as A) the nanoindentation load-displacement curve for the PES electrospun nanofibrous mats; B) the dynamic compressive properties including compaction index and storage modulus; C) variation of displacement at hold segment of load representative of creep of the PES electrospun nanofibrous mats

Figure 4. Tensile test results as A) stress- strain curves for the PES electrospun nanofibrous mats; B) the tensile properties including elastic modulus, tensile strength and elongation

Figure 5. Pore size measurement of the PES ENMs

Figure 6. Permeation performance of the PES ENMs at various feed pressures

Figure 7. SEM micrographs showing the surface of the PES ENMs before and after water flux test under a 2 bar feed pressure for the PES ENMs as (A,B) untreated and (C,D) heat treated

Figure 8. Retention performance (A) and permeability (B) of the PES ENMs at various feed pressures evaluated by using TiO₂ aqueous suspensions

Figure 9. SEM micrographs showing the cake layer formation on the surface of the PES ENMs after a retention test using TiO₂ aqueous suspensions at various feed

pressures A) HPES (1 bar); B) HPES (2 bar); C) PES (1 bar); D) PES (2 bar) (the circle show a single nanofiber remained after disintegration)

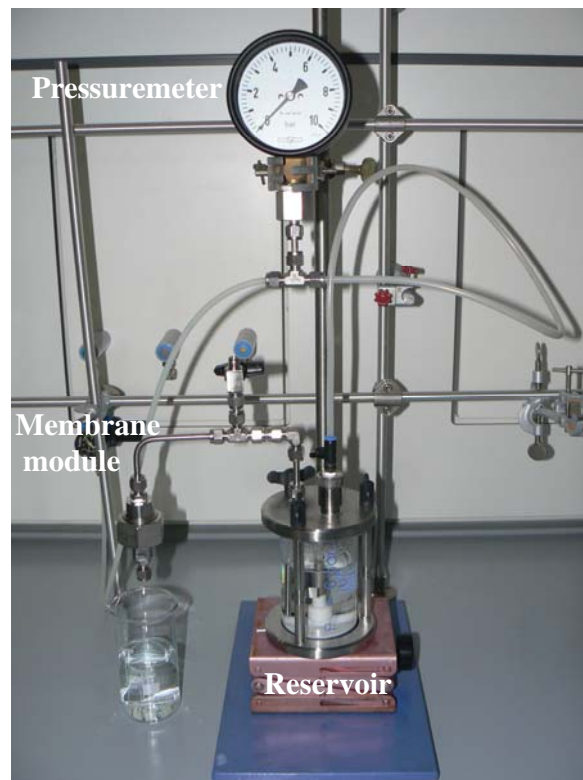


Fig. 1

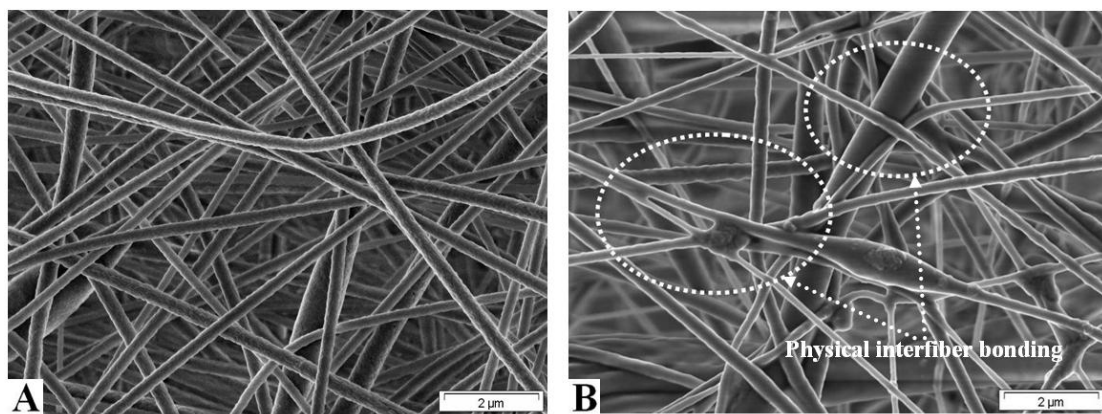
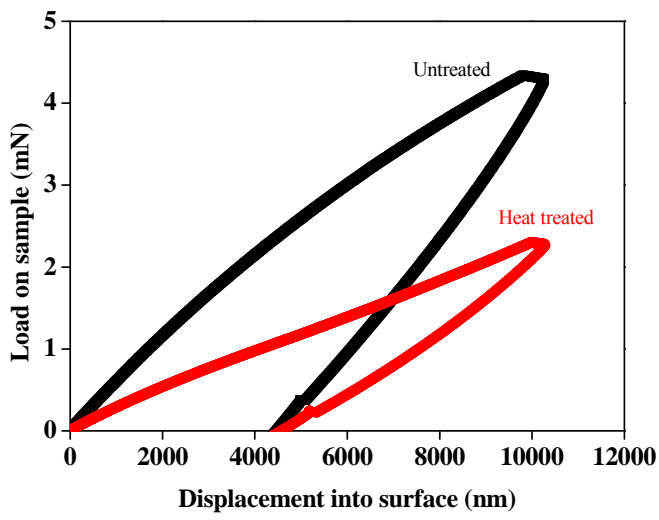
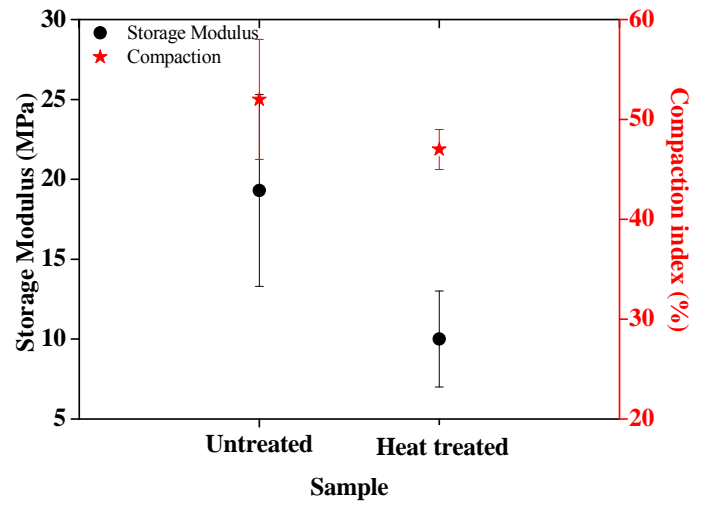


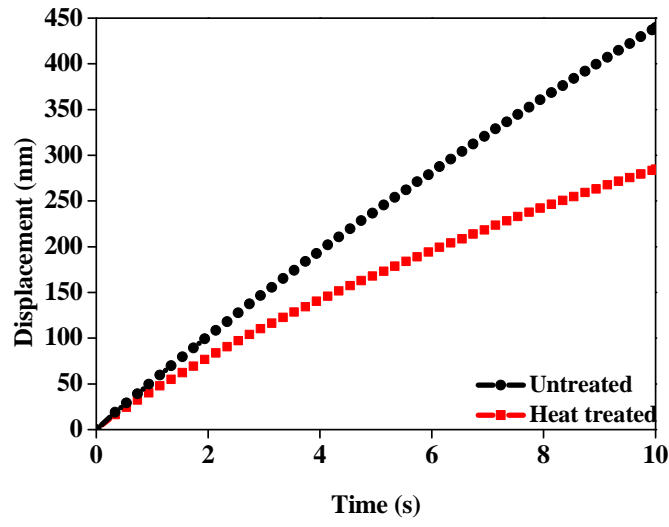
Fig. 2



(A)

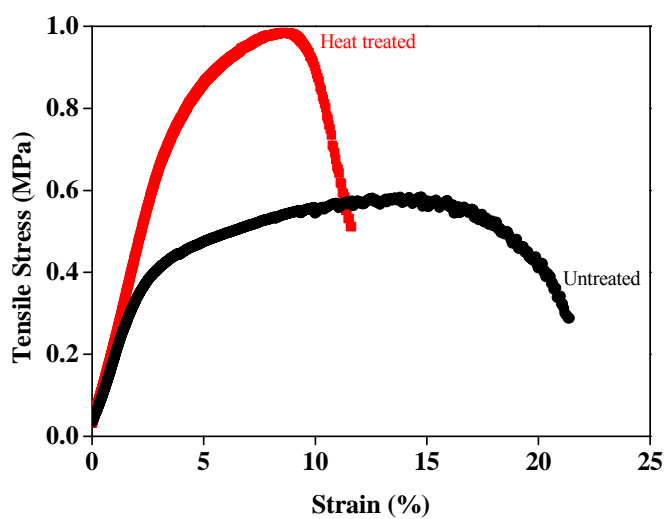


(B)

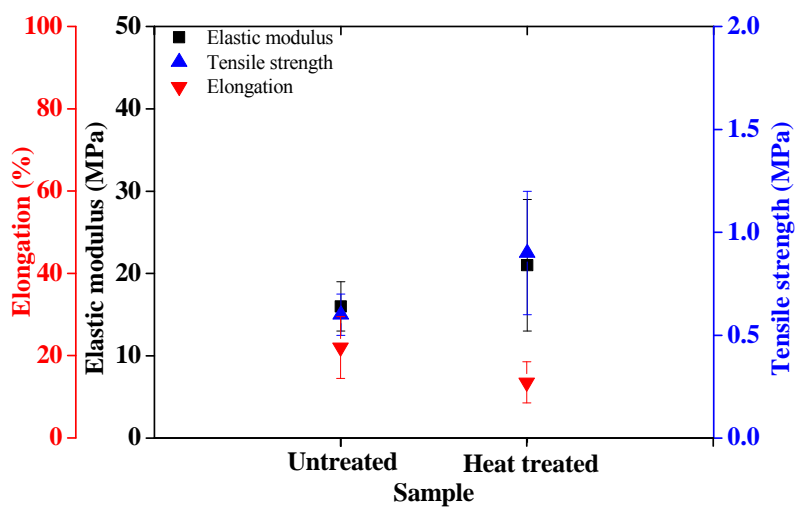


(C)

Fig. 3



(A)



(B)

Fig. 4

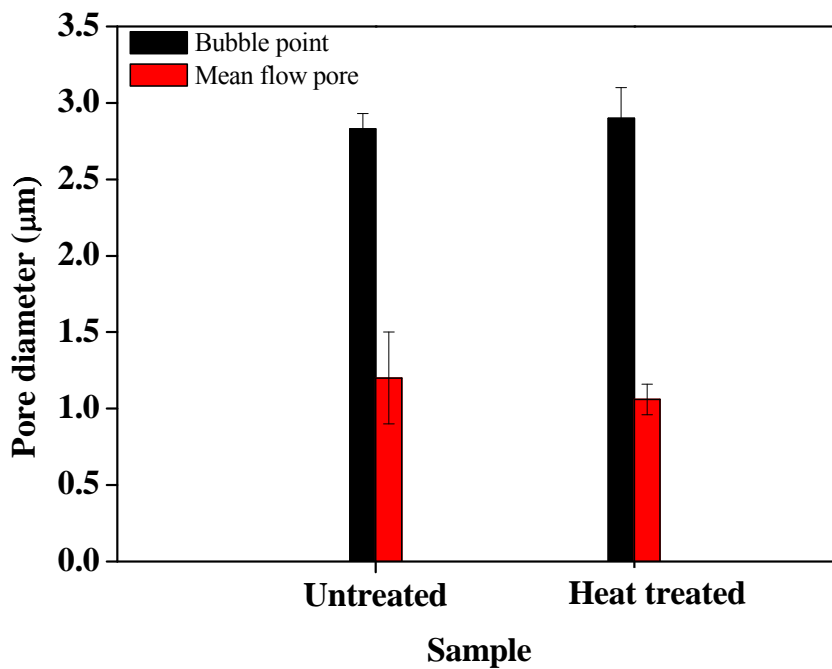


Fig. 5

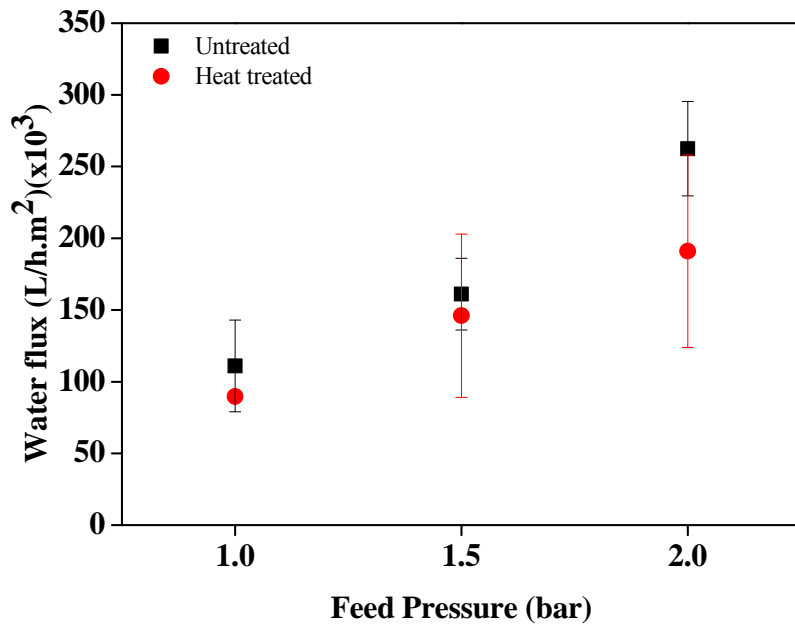


Fig. 6

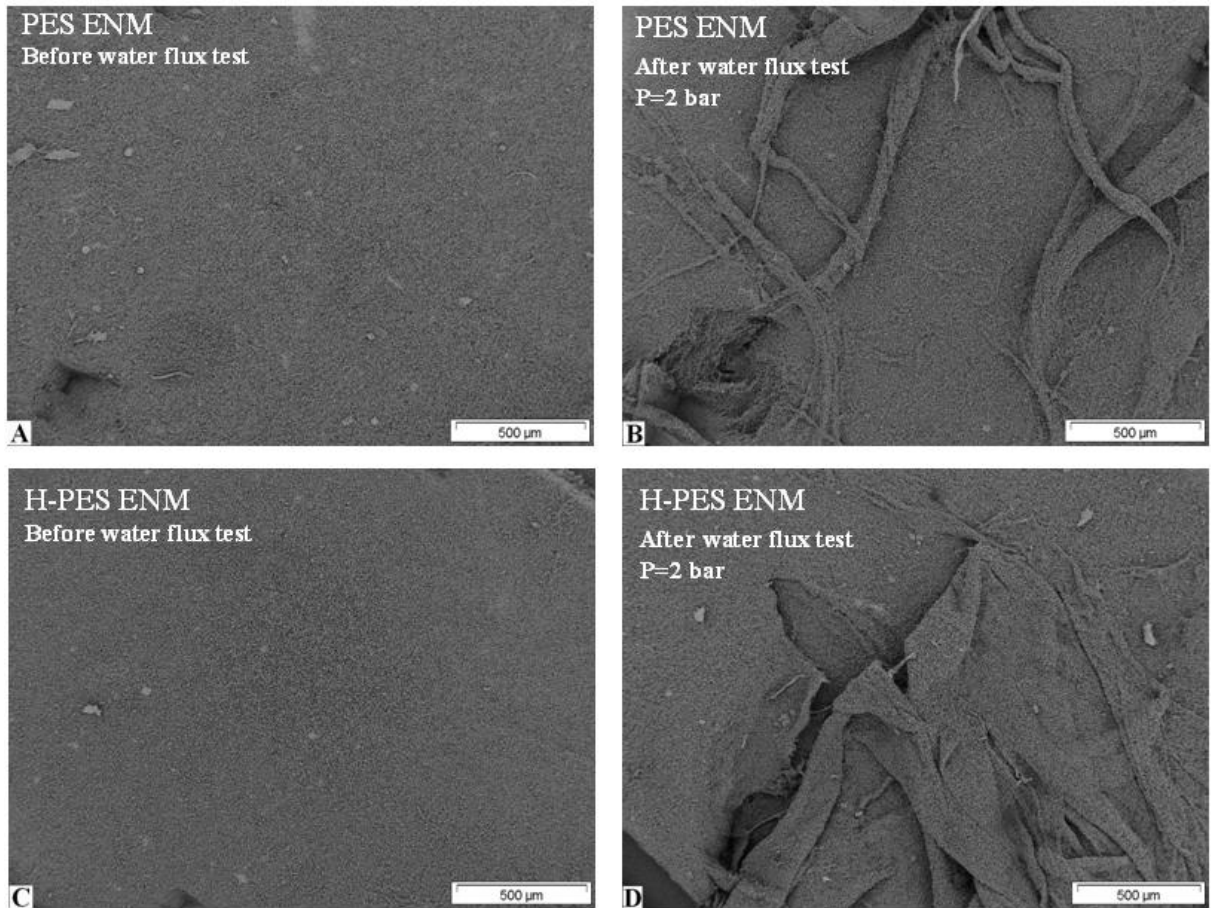
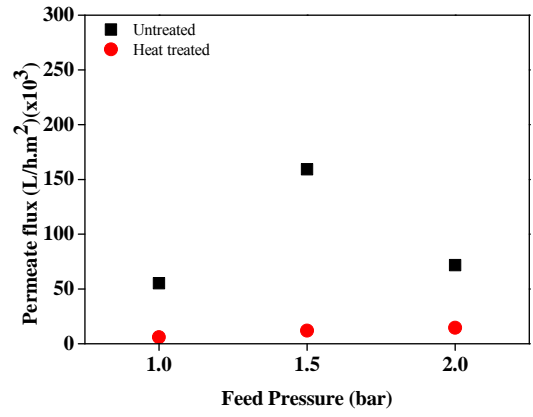
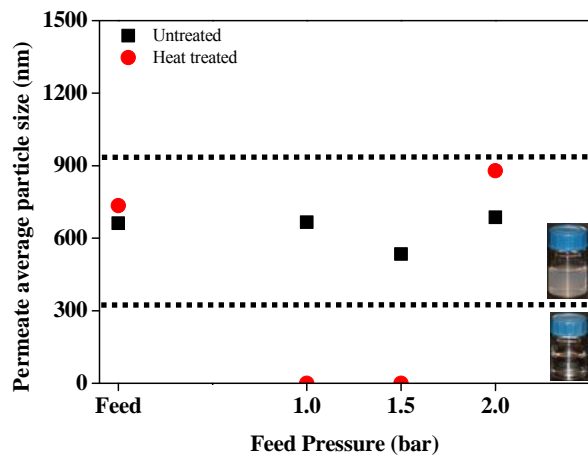


Fig. 7



(A)

(B)

Fig. 8

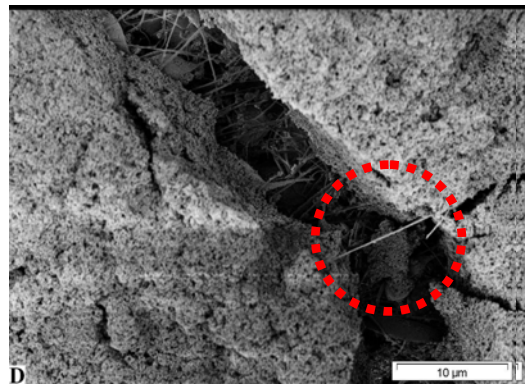
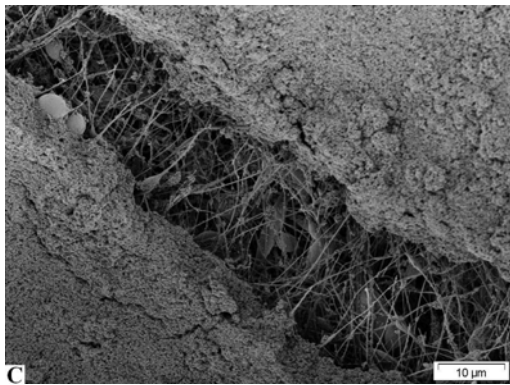
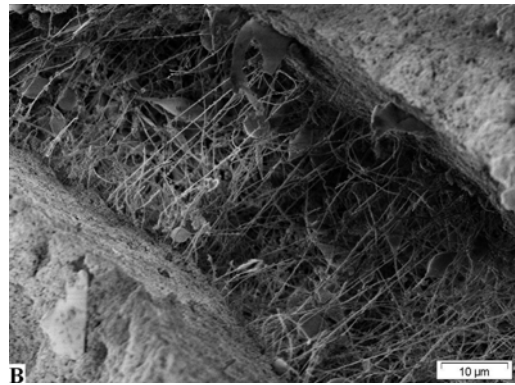
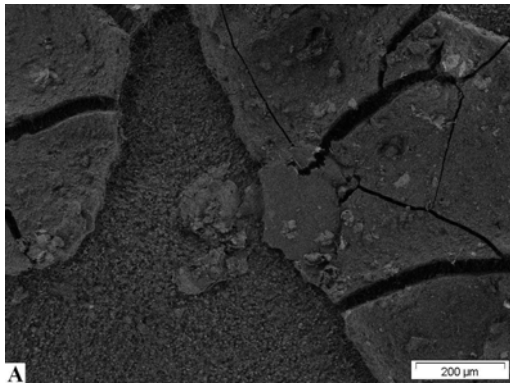


Fig. 9